Infrared study of superconductivity in $YBa_2(Cu_{1-x}M_x)_3O_{7-\delta}$ (M = Zn and Ni)

Jin-Tae Kim and Thomas R. Lemberger
Department of Physics, The Ohio State University, Columbus, Ohio 43210

Steve R. Foltyn and Xindi Wu
Los Alamos National Laboratory, Los Alamos, New Mexico 87545

(Received 1 February 1994)

We report the infrared reflectances $R(\nu,T)$ of $YBa_2(Cu_{1-x}M_x)_3O_{7-\delta}$ films (M = Zn and Ni) for frequencies 50 cm^{-1} < ν < 1000 cm^{-1} and temperatures T = 10, 100, and 300 K. The "best fit" conductivities, $\sigma_1(\nu,10\text{ K})$, for both Zn- and Ni-doped films show no clear evidence of superconductivity, i.e., the superconducting density of states is very gapless. This degree of gaplessness is consistent with the large penetration depths measured in the same films. It agrees with estimates based on the measured carrier scattering rate $1/\tau$ (10 K) and theories of d-wave superconductors. The carrier scattering rate $1/\tau(T)$ increases with dopant concentration x and with T; it does not change rapidly just below T_c as in pure $YBa_2Cu_3O_{7-\delta}$. The plasma frequency $\omega_p = 8500 \pm 500$ cm^{-1}, independent of dopant concentration and T, agrees with values obtained in pure $YBa_2Cu_3O_{7-\delta}$.

The most interesting issue in the infrared properties of high-T_c superconductors is the origin and nature of the superconducting state. There is a growing body of evidence that the density of states in high-T_c superconductors is not zero for energies less than a few kT_c, as in conventional superconductors. It is merely suppressed somewhat below its normal-state value.[1-3] In conventional superconductors, such "gaplessness" could indicate anisotropy in the order parameter arising from an anisotropic electron-boson coupling, or from pair breaking from a small concentration of magnetic impurities. In oxide superconductors, it is proposed that the anisotropy reflects the d-wave symmetry of the order parameter.[4-8] Because d-wave models have enjoyed some success in describing the properties of pure $YBa_2Cu_3O_{7-\delta}$ (YBCO), and a hallmark of d-wave superconductors is their extreme sensitivity to elastic scattering of the carriers, it is interesting to study the evolution with doping of the infrared reflectance of Zn-doped YBCO, and to compare the results with d-wave models.

The effect of elastic scattering is dramatically different for conventional s-wave and unconventional d-wave superconductors. In a clean d-wave superconductor, the density of states $N_S(E)$ is gapless; it increases linearly from zero at $E=0$ and has a logarithmic singularity at the "gap" energy $\Delta_0(T)$. Elastic scattering from strongly scattering impurities shifts quasiparticle states from energies near Δ_0 into an "impurity band" which is centered at or near $E=0$, thereby making $N_S(E)$ even more gapless. As the scattering rate exceeds $\Delta_0/\hbar$, $N_S(0)$ approaches its normal-state value. By contrast, in clean conventional s-wave superconductors, intrinsic anisotropy in the order parameter due to anisotropic electron-phonon interactions rounds off the BCS singularity in N_S and allows some states to exist at energies below the energy of the peak in N_S, i.e., in the gap. Thus, the actual energy gap can be well below the "average gap," and the superconductor can appear nearly gapless in some measurements. However, elastic scattering reduces order-parameter anisotropy so that $N_S(E)$ becomes more BCS-like, with a clearly defined gap, rather than more gapless.

Our earlier study[1] of Ni-doped YBCO and the study of Mandrus *et al.*[2] of irradiation-damaged $Bi_2Sr_2CaCu_2O_8$ established gaplessness of the superconducting density of states in these disordered oxide superconductors. Our purposes in the present study are to compare the effects of Ni and Zn doping and to explore more carefully the evolution of the superconducting state with increasing disorder. Acquisition of a low-noise infrared detector improves our data over our previous study of Ni-doped YBCO, so we include new data on a Ni-doped film.

The comparison between Zn- and Ni-doped YBCO is interesting. Ni and Zn are the only Cu dopants for which there is substantial evidence for substitution in the CuO_2 planes; other dopants like Al, Co, and Fe prefer the CuO chain sites. Precise site occupation probabilities are controversial, but it seems that both substitute into plane and chain sites with equal probabilities, although Zn may have a slight preference for plane sites while Ni has a slight preference for chain sites.[9] Both are in +2 charge states. Both suppress T_c rapidly, although Zn suppresses T_c at a rate (10 K/at. %) about twice that of Ni. The dc resistivities[10] of Ni-doped films indicate that Ni increases the scattering rate $1/\tau$ more than Zn. Even though Zn^{2+} is spin 0 ($3d^{10}$) while Ni^{2+} is spin 1 ($3d^8$), when they substitute for spin-$\frac{1}{2}$ Cu both may induce local magnetic moments in the lattice. A recent NMR study of Zn-doped YBCO concludes that there is indeed a local magnetic moment associated with each Zn atom, but that its coupling to the conduction carriers is too weak to account for the suppression in T_c within the theory of magnetic impurities in conventional superconductors.[11] A similar study on Ni-doped YBCO would be interesting. In a measurement of direct relevance to the current study, a

recent microwave study of the surface resistance of doped YBCO crystals finds that Zn creates an impurity band near $E=0$ and Ni does not, at least at concentrations below 1%.[12] In contrast, we find that the qualitative effects of Zn and Ni are the same, namely, both induce strong gaplessness in the superconducting density of states, at least at concentrations above 1%.

The Zn-doped YBCO films were made by *in situ* laser ablation from a stoichiometric ceramic target onto heated (100) $SrTiO_3$ substrates at Los Alamos National Laboratory. The 6% Ni-doped YBCO film was fabricated in the same way as films from previous work;[10] codeposition of Y, BaF_2, Cu, and Ni onto a room-temperature (100) $SrTiO_3$ substrate, with a postanneal at 900 °C in flowing oxygen. The films were about 1.5 cm in diameter and 250, 290, and 300±10 nm thick, respectively, for 2% Zn, 4% Zn, and 6% Ni. The thicknesses of the Zn-doped films were measured by Rutherford backscattering. The thickness of the 6% Ni film was measured with an α-step profilometer. The same Zn-doped films used for the infrared studies were later patterned for the resistivity measurements. The fact that the influence of dopants seems to be independent of the technique used to make the film supports the notion that the electrodynamic properties of the films are not unduly influenced by grain boundaries and other flaws that likely are sensitive to fabrication method.

The high-resolution reflectance spectra were taken with a bolometer for $50<\nu<1500$ cm^{-1} and a Bomem Corporation Fourier transform spectrometer. The film and a Au mirror were mounted several centimeters apart on a cold finger. The reflectance of the sample relative to Au was measured by raising and lowering the cold finger, thereby moving the two films in and out of the optical path. When Au mirrors were mounted at both locations on the cold finger, one position had a reflectance that was reproducibly 0.005 higher than the other even when the Au mirrors were switched, and we corrected for this in our data. We assume that the reflectance of Au in the infrared is 1.00. Our reflectances are accurate to ±0.005 and have a precision of ±0.001. Spectra taken over different frequency ranges with different beam splitters and/or detectors overlap to better than 0.005.

After the infrared measurements, the Zn-doped films were patterned into strips for resistivity measurements (Fig. 1), which show sharp transitions. The $\rho(T)$ are only about 15% larger for all temperatures than measured in Zn-doped crystals.[13] The dotted lines in Fig. 1 suggest that the residual resistivity increases with Zn concentration. The estimated residual resistivity is about double the value inferred from the infrared measurements, as discussed below.

The inductive transition temperatures, determined from the mutual inductance of coils on opposite sides of the unpatterned films, are 62, 42, and 70 K, respectively, for 2% Zn, 4% Zn, and 6% Ni, and the transition widths are about 2 K. The inductive T_c's are near where the resistivity vanishes (Fig. 1). The transition widths are about equal to the difference between the mean-field and Kosterlitz-Thouless transition temperatures, where the latter is estimated from the measured penetration

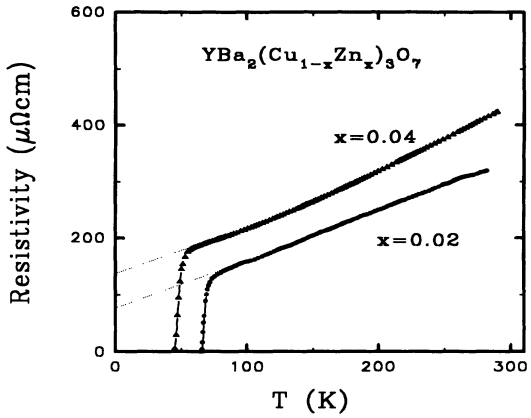

FIG. 1. Resistivities vs T of 2% and 4% Zn-doped $YBa_2(Cu_{1-x}Zn_x)_3O_{7-\delta}$ films. Residual resistivities are suggested by dotted lines.

depths.[14] The 2-K transition widths indicate good film homogeneity. For comparison, if the concentration of Zn in the 4% Zn film varied by ±10% from 3.5% to 4.5% throughout the film, then the transition width would be at least 10 K just from the different suppressions in T_c.

From the inductance measurements, the penetration depth $\lambda(T=0)$ in the *ab* plane is about 350 and 900 nm respectively for 2% and 4% Zn-doped films, and about 800 nm for the 6% Ni-doped film.[14] Thus, $1/\lambda^2(0)$ is about 5–30 times smaller than for pure $YBa_2Cu_3O_{7-\delta}$. The large penetration depths have important implications for the infrared. Because the area "missing" from $\sigma_1(\omega)$ in the superconducting state at $T=0$ is $\pi/2\mu_0\lambda^2(0)$, the large penetration depths are consistent with the essentially "normal" behavior that we observe, i.e., little, if any, area missing from $\sigma_1(\omega)$, as described below.[15–17]

Figure 2 shows the infrared reflectances at 10, 100, and 300 K of Zn- and Ni-doped $YBa_2Cu_3O_{7-\delta}$ films on $SrTiO_3$ substrates, together with model calculations (bold curves) described below. There are prominent features at about 80, 180, and 540 cm^{-1} from phonons in the substrate, which are included in our modeling. These features indicate that the light probes the entire film thickness. There are many small sharp features, from phonons in the film, which are not included in the modeling. Spectra taken with different beam splitters, etc., overlap nicely, for example, at about 325 cm^{-1}. We do not make any adjustments to fit different spectra together.

For all three doped films, the reflectance rises monotonically as temperature decreases. Substrate features diminish as less radiation penetrates through the film. As T decreases from 300 to 100 K, the 80-cm^{-1} substrate phonon moves below 50 cm^{-1} and is responsible for the downturn in the reflectances at 10 K for $\nu<100$ cm^{-1}. At 10 K, the far-infrared reflectance ($\nu<200$ cm^{-1}) is largest for 2% Zn and smallest for 6% Ni, indicating that absorption correlates better with the concentration of dopant than the reduction of T_c, since the 6% Ni-doped film has a higher T_c than the 2% Zn-doped film. Be-

tween 100 and 10 K, the reflectance rises smoothly; no sharp features develop which would indicate the presence of a superconducting gap.

The similarity of the superconducting-state reflectances at 10 K to the normal-state reflectances at 100 K for all three films suggests that the infrared conductivities at 10 K cannot be much different from what they would have been if superconductivity had not occurred, and this is borne out by numerical modeling of the spectra. Following Sumner, Kim, and Lemberger,[1] the sample is modeled as a film on an infinitely thick $SrTiO_3$ substrate, and the dielectric function of $SrTiO_3$ is taken from the literature. There is some variation from substrate to substrate evident in the slightly different frequencies of the strong phonons, particularly the phonon at 540 cm^{-1}, so we make minor adjustments as needed to fit these features. We have checked that approximating the 1-mm-thick substrate with an infinitely thick substrate is justified numerically, given the 4-cm^{-1} resolution at which we run the spectrometer.

The conductivity of the $YBa_2Cu_3O_{7-\delta}$ film is modeled with two components. The first component represents conduction carriers, and it is a Drude conductivity, $\sigma_1(\omega)=\varepsilon_0\omega_p{}^2\tau/(1+\omega^2\tau^2)$, characterized by a plasma frequency ω_p and a scattering rate $1/\tau(T)$. Above T_c, in the limit of $\omega\to 0$, $\sigma_1(\omega,T)$ should approach $1/\rho(T)$, the dc resistivity. The second component of the conductivity of the film is a midinfrared band of bound carriers of uncertain origin, which we model following Kamaras *et al.*[18] with three Lorentzians. As discussed below, the midinfrared band develops a weak peak at 300 cm^{-1} upon cooling from 300 to 100 K, but does not change perceptibly between 100 and 10 K.

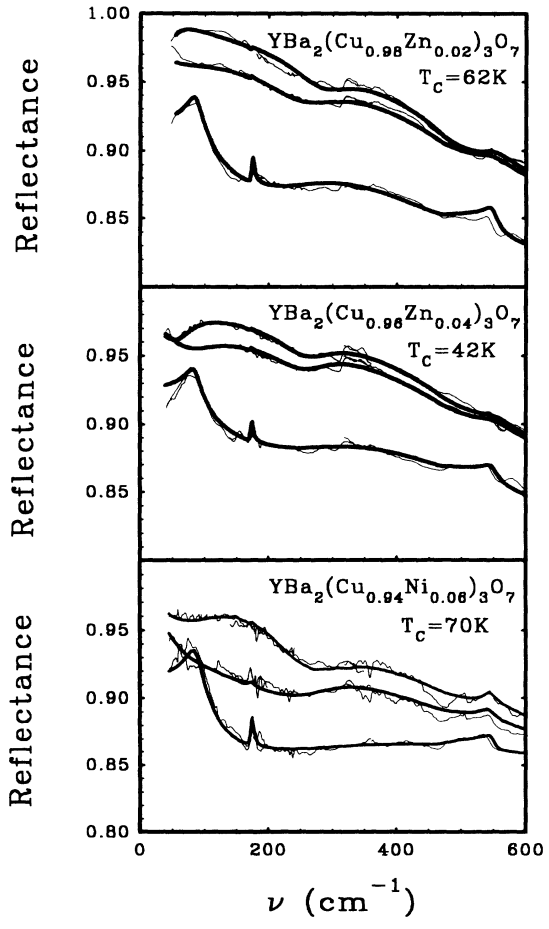

FIG. 2. Far-infrared reflectances of 2% and 4% Zn-doped and 6% Ni-doped $YBa_2(Cu_{1-x}M_x)_3O_{7-\delta}$ films at 10, 100, and 300 K. Thick solid curves are model calculations from the conductivities in Fig. 3. Details of the fitting procedures are in the text.

The fitting procedure used at 100 and 300 K is the following. First we fix the nine parameters associated with the midinfrared band, using the values determined by Kamaras *et al.*,[18] and adjust the Drude parameters ω_p and $1/\tau$ to get a good fit to the measured reflectance. Then we fix the Drude parameters and adjust all nine midinfrared band parameters to improve the fit. Then we readjust the Drude parameters, and so on. After a few iterations, the procedure converges to an excellent "best fit," as seen in Fig. 2. Deviations below about 100 cm^{-1} are likely from deviations of the substrate dielectric function from the literature value for $SrTiO_3$.

Figure 3 shows the total conductivities $\sigma_1(\nu,T)$, which correspond to the calculated reflectances (thick solid curves) in Fig. 2. It is clear that σ_1 develops a Drude peak at $\nu=0$ as the film cools from 300 to 100 K, as expected from the measured decrease in resistivity. The "Drude" peak gets higher and narrower in the superconducting state.

The insets to Fig. 3 show the midinfrared component of σ_1 at 300 and 100 K. The midinfrared band changes very little from 300 to 100 K; mainly it develops a small peak at about 300 cm^{-1}. This peak describes the weak broad maximum in R near 300 cm^{-1} that develops at 100 K, and it has been reported by others[19] in $YBa_2Cu_3O_{7-\delta}$.

The best-fit values of ω_p, $1/\tau$, and $\rho=1/\sigma_1(\nu=0)$ are collected in Table I. Values for the 10-K data result from fitting these superconducting-state data with a purely normal Drude conductivity. Since the fit is reasonably good, these values are significant. ω_p varies somewhat from temperature to temperature and sample to sample. However, considering the uncertainties in the data and the separation of the conductivity into components, we hesitate to assign any physical significance to these variations. We conclude that $\omega_p=8500\pm500$ cm^{-1} (1.05 eV), independent of T and dopant concentration. This range of values agrees with that of Kamaras *et al.* who use the same two-component model in analyzing the reflectance data of their YBCO films.[18] We discuss the scattering rate $1/\tau$ below. The value of $\rho=1/\sigma_1(\nu=0,T=100\text{ K})$ in Table I is about 50% smaller than the dc resistivity $1/\rho(100\text{ K})$ for the Zn-doped films. Since this sort of discrepancy is commonly observed in infrared spectra, including a study of 4% Ni-doped films,[1] it is bothersome, but not of deep concern here.

The model fits the data at 100 and 300 K very well, especially for $\nu<300$ cm^{-1} where the Drude conductivity dominates over the midinfrared band. This shows that the model accurately describes the conduction carriers in

the frequency range where the superconducting gap should appear. The accuracy of the conductivity obtained from the best fit does not depend on the assumption that the conductivity can be expressed as two components.

The 10-K data require two fitting procedures, the first of which neglects superconductivity completely. The first procedure uses a Drude conductivity to describe the conduction carriers and it uses the midinfrared band determined at 100 K on the same film. The best-fit conductivity is shown as the long-dashed curves in Fig. 3; the corresponding reflectance curve is not shown in Fig. 2. The quality of the fit is similar to that discussed in detail by Sumner, Kim, and Lemberger[1] in their analysis of a 4% Ni-doped film: the fit is acceptable, but misses some changes in slope of the reflectance at a couple of frequencies. The purpose of this fitting procedure is to highlight how close the reflectance at 10 K is to that of a completely normal conductor. Moreover, the width of the "Drude" peak shows that $1/\tau(10\ \mathrm{K})$ is comparable to $kT_c/\hbar$, so that a drop in reflectance of about 0.08 would occur at 2Δ if there were a BCS-like gap in the optical conductivity.[1]

TABLE I. Drude parameters at $T=300$, 100, and 10 K for 2% and 4% Zn-doped and 6% Ni-doped YBCO films: plasma frequency $\omega_p(\mathrm{cm}^{-1})$, resistivity $\rho=1/\sigma_1(\nu=0)$ ($\mu\Omega$ cm), and scattering rate $1/\tau$ (cm^{-1}).

Dopant	T (K)	Plasma frequency ω_p (cm^{-1})	Resistivity $\rho(\mu\Omega\,\mathrm{cm})$	Scattering rate $1/\tau$ (cm^{-1})
2% Zn	300	8000	310	330
	100	9000	90	120
	10	9000	45	53
4% Zn	300	8000	320	340
	100	8700	110	139
	10	8700	70	88
6% Ni	300	8200	440	493
	100	8200	220	246
	10	8200	125	140

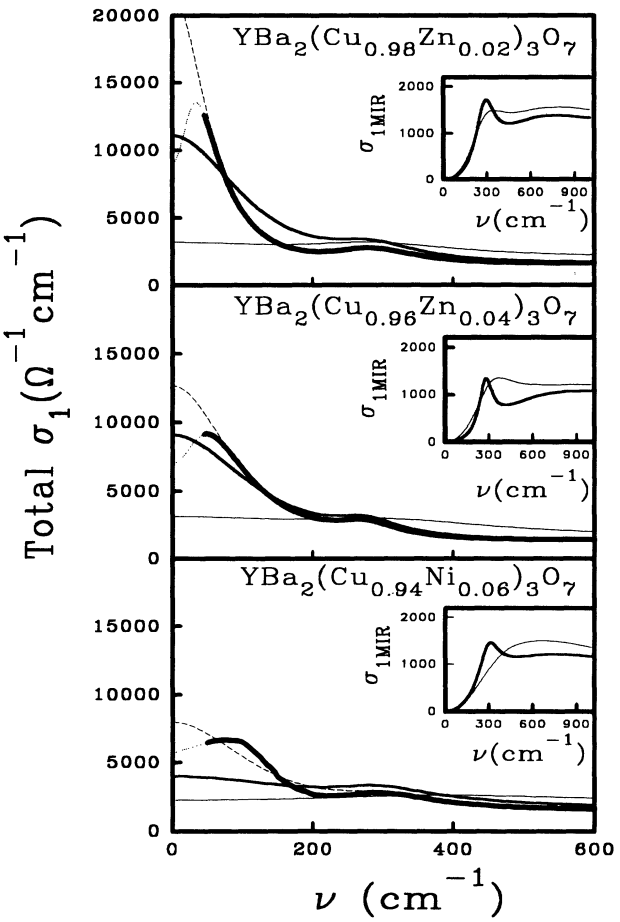

FIG. 3. Best-fit total conductivities of 2% and 4% Zn-doped and 6% Ni-doped $YBa_2(Cu_{1-x}M_x)_3O_{7-\delta}$ films for 10- (thick solid curve), 100- (thin solid curve), and 300-K (thinner solid curve) reflectance spectra in Fig. 2. The long-dashed curves for $\nu<50\ \mathrm{cm}^{-1}$ are best fits to the 10-K spectra from a procedure that neglects superconductivity; the light-dotted lines are extrapolations of best fits from a procedure that includes superconductivity. The area between the long-dashed and light-dotted curves corresponds to the measured penetration depth λ ($T=0$ K). The insets shows the respective midinfrared bands.

The second fitting procedure for the 10-K reflectances includes superconductivity in $\sigma_1(\nu)$ as a δ function at $\nu=0$ and a "modified Drude" conductivity for $\nu>0$. It uses the midinfrared band determined at 100 K. The "modified Drude" conductivity is obtained by adjusting the Drude conductivity found in the first fitting procedure to get a better "best fit." The very good fits at 10 K shown in Fig. 2 are from this fitting procedure with δ functions corresponding to measured penetration depths. It is impossible to fit the 10-K data when the δ function in σ_1 corresponds to a penetration depth that is too short, i.e., $\lambda<300$, 500, and 500 ± 100 nm for 2% Zn, 4% Zn, and 6% Ni, respectively, because the calculated reflectances are too high. These lower-limit values of λ are quite close to direct measurements[14] of λ. We extrapolate $\sigma_1(\nu,10\ \mathrm{K})$ to $\nu<50\ \mathrm{cm}^{-1}$, shown by the light-dotted line in Fig. 3, in a way that the "missing area" between the "superconducting" and the "normal" conductivities corresponds to the values of λ just quoted. Thus, the far-infrared conductivity $\sigma_1(\nu,10\ \mathrm{K})$ lies somewhere between the extremes set by the two fitting procedures, and probably is closer to the second fit.

It is immediately clear from the two best-fit conductivities at 10 K (Fig. 3) that there is very little evidence for superconductivity. If there is any significant suppression in the low-frequency conductivity below its normal-state value, then it occurs below 70 cm^{-1} where substrate effects limit our resolution. For reference, a BCS-like gap feature at $3.5kT_c$ for $T_c=60$ K would appear as a drop of 0.08 in R at $\nu_g=146\ \mathrm{cm}^{-1}$. There is no qualitative difference among 2% and 4% Zn and 6% Ni doping, except that the 2% Zn conductivity is highest and narrowest, as expected from the lower scattering rate deduced from the resistivity. It would be interesting to study lower dopant concentrations, but there is the tech-

nical problem that the reflectance even for 2% Zn is so close to unity that the 0.005 uncertainty in the reflectance will become quite significant for lower Zn concentrations.

There are a number of theories of superconductivity that include gaplessness in the density of states with or without disorder, including *d*-wave theories[3,4] and marginal Fermi liquid theories.[20] *d*-wave theories have the attractive feature that disorder is naturally accommodated and need not be added in an *ad hoc* fashion. Hence we concentrate our analysis on a comparison with *d*-wave theories. It will be interesting to compare our data with the other theories when calculations are available.

Theory indicates that the evolution of the conductivity of a *d*-wave superconductor with disorder should be hard to observe. In *d*-wave models with no disorder, $1/\tau \rightarrow 0$, even the normal state is perfectly reflecting because the Drude conductivity is essentially a δ function at $\nu=0$, just like a superconductor. When disorder reaches a level where the scattering rate is comparable to the order parameter Δ, so that the reflectance of a BCS superconductor would drop by several percent at $h\nu=2\Delta$, the density of states of a *d*-wave superconductor is already considerably smeared by the disorder, and superconducting features in the conductivity $\sigma_1(\nu)$ are smeared and softened. Calculations on *d*-wave superconductors[3] with line nodes in the order parameter, which are equivalent to *p*-wave calculations[21] with line nodes, indicate that one can hope to observe at relatively small disorder that $\sigma_1(\nu)$ is suppressed below its normal-state value only below $\nu \cong 2kT_{c0}/h \cong 125$ cm^{-1}, which is several times smaller than the frequently used value $2\Delta_0(0)/h \cong 6kT_{c0}/h$, where T_{c0} is 90 K. The absence of any significant sharp suppression of $\sigma_1(\nu)$ for $\nu < 150$ cm^{-1}, even for our lowest doping level of 2% Zn, is therefore not surprising and in agreement with what is known theoretically about the conductivity of *d*-wave superconductors.

Measurements[22,23] on pure YBCO and $Bi_2Sr_2CaCu_2O_8$ indicate that the scattering rate drops rapidly just below T_c, suggesting either that a BCS-like gap opens in the density of states or that the interaction (spin fluctuations, perhaps) responsible for inelastic scattering is suppressed by superconductivity. Hence, it is interesting to see whether the scattering rate drops by a similar amount in doped films. To this end, we measured the reflectance of the 2% Zn film for $50 < \nu < 200$ cm^{-1}, at 10-K intervals from 10 to 100 K. Reflectances at 10 and 100 K are close for $\nu > 300$ cm^{-1}, so this ν range is sufficient to determine $1/\tau$.

The reflectance rises smoothly as T decreases. There is no evidence for an abrupt change near T_c. Correspondingly, the fitted scattering rate $1/\tau$ decreases smoothly as

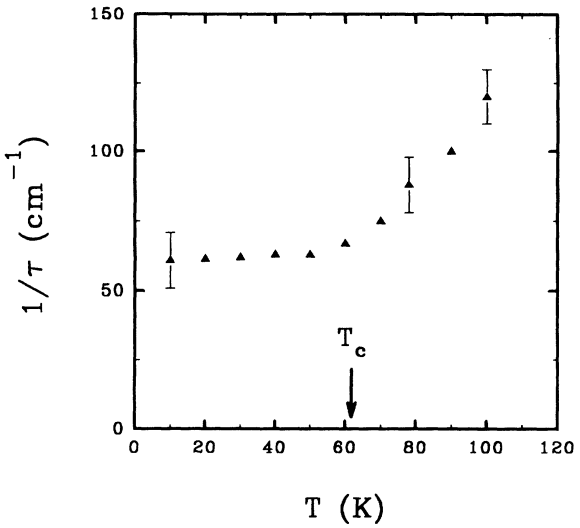

FIG. 4. Scattering rate $1/\tau(T)$ of the $YBa_2(Cu_{0.98}Zn_{0.02})_3O_{7-\delta}$ film. At each temperature, the error bar is the same. For reference, 100 cm^{-1} = 1.9×10^{13}/s = 150 K.

T decreases. It is linear for $T \geq T_c$ and constant below T_c, as shown in Fig. 4. There is no indication of a drop in $1/\tau$ near T_c. For pure YBCO, $1/\tau$ drops by about 80 cm^{-1} within about 15 K below T_c, and such a drop would be very clear with our resolution.

In summary, the infrared conductivities of 2% and 4% Zn-doped and 6% Ni-doped YBCO films show no evidence of superconductivity at temperatures well below T_c, i.e., the superconducting density of states is not much different from its normal-state value. The idea that grain boundaries do not contribute significantly is supported by the fact that the resistivities of Zn-doped films are only slightly higher than Zn-doped crystals, and that the reflectances are insensitive to the films fabrication procedure. This conclusion of gaplessness is supported by other measurements. Ulm, Kim, and Lemberger[14] find that penetration depths $\lambda(T)$ of the same doped films reported herein are large, consistent with the nearly normal infrared conductivity. The nonzero value of $N_S(0)$ is also evident as a linear-in-T electronic specific heat of Zn-doped YBCO,[24] as well as in the convolved density of states derived from photoemission data.[25] Thus, disorder-induced gaplessness is well established in YBCO at least. This does not rule out other models, but is strong support for *d*-wave models.

This work was supported primarily by NSF-DMR 92-00870. We are grateful to Gordon Thomas and Thomas Timusk for insightful comments on the manuscript.

[1]M. J. Sumner, J.-T. Kim, and T. R. Lemberger, Phys. Rev. B **47**, 12 248 (1993).
[2]D. Mandrus *et al.*, Phys. Rev. Lett. **70**, 2629 (1993).
[3]C. Jiang and J. P. Carbotte (unpublished).
[4]P. Monthoux, A. V. Balatsky, and D. Pines, Phys. Rev. Lett. **67**, 3448 (1991).
[5]N. Bulut and D. J. Scalapino, Phys. Rev. Lett. **68**, 706 (1992).
[6]E. J. Nicol, C. Jiang, and J. P. Carbotte, Phys. Rev. B **47**, 8131 (1993).
[7]Z.-X Shen *et al.*, Phys. Rev. Lett. **70**, 1553 (1993).
[8]D. A. Wollman *et al.*, Phys. Rev. Lett. **71**, 2134 (1993).
[9]L. H. Greene and B. G. Bagley, in *Physical Properties of High*

Temperature Superconductors, edited by D. M. Ginsberg (World Scientific, New York, 1990), Vol. II, p. 509.
[10]J.-T. Kim, D. G. Xenikos, A. Thorns, and T. R. Lemberger, J. Appl. Phys. **72**, 803 (1992).
[11]R. E. Walstedt *et al.*, Phys. Rev. B **48**, 10 646 (1993).
[12]D. A. Bonn *et al.* (unpublished).
[13]T. R. Chien, Z. Z. Wang, and N. P. Ong, Phys. Rev. Lett. **67**, 2088 (1991).
[14]E. R. Ulm, J.-T. Kim, and T. R. Lemberger (unpublished).
[15]J.-T. Kim, M. J. Sumner, E. R, Ulm, and T. R. Lemberger, J. Phys. Chem. Solids **54**, 1335 (1993).
[16]J.-T. Kim, E. R. Ulm, and T. R. Lemberger, Physica B **194-196**, 1535 (1994).
[17]E. R. Ulm, J.-T. Kim, and T. R. Lemberger, Physica B **194-196**, 2331 (1994).
[18]K. Kamaras *et al.*, Phys. Rev. Lett. **64**, 84 (1990).
[19]D. B. Tanner and T. Timusk, in *Physical Properties of High Temperature Superconductors,* edited by D. M. Ginsberg (World Scientific, New York, 1991), Vol. III, p. 363.
[20]P. B. Littlewood and C. M. Varma, Phys. Rev. B **46**, 405 (1992).
[21]P. J. Hirschfeld *et al.*, Phys. Rev. B **40**, 6695 (1989).
[22]D. A. Bonn, P. Dosanjh, R. Liang, and W. N. Hardy, Phys. Rev. Lett. **68**, 2390 (1992).
[23]D. B. Romero *et al.*, Phys. Rev. Lett. **68**, 1590 (1992).
[24]J. W. Loram, K. A. Mirza, and P. F. Freeman, Physica C **171**, 243 (1990).
[25]G. B. Arnold, F. M. Mueller, and J. C. Swihart, Phys. Rev. Lett. **67**, 2569 (1991).